Catalysis Science & Technology

Accepted Manuscript

ROYAL SOCIETY OF CHEMISTRY

www.rsc.org/catalysis

Journal Name

RSCPublishing

ARTICLE

Rational design of carbon support to prepare ultrafine-iron-oxide catalyst for air oxidation of alcohols†

Cite this: DOI: 10.1039/xoxxoooooox

Longlong Geng,[a] Min Zhang,[a] Wenxiang Zhang,[a] Mingjun Jia,[a] Wenfu Yan [b] and Gang Liu*[a]

Received ooth January 2012,
Accepted ooth January 2012

DOI: 10.1039/xoxxoooooox

www.rsc.org/

A kind of mesoporous carbon supports with abundant surface functional groups and tunable pore size were prepared using a modified hard-template route. They were demonstrated to be efficient supports for fabricating ultrafine-iron-oxide catalysts, and the resultant catalysts exhibit an obviously higher activity in air oxidation of several benzyl alcohols compared with the catalysts with other synthetic carbon as supports. The concrete role of carbon support in the catalyst design was investigated in detail. The negatively charged surface oxygen functional groups serve as strongly active sites for anchoring positively charged Fe^{3+} ions and lead to high dispersion of iron oxide species. These oxygen functional groups also provide a suitable coordinate environment to increase the electron density of iron centres and form efficient active sites for the oxidation of benzyl alcohols with molecular oxygen.

Introduction

Catalytic oxidation of alcohols and carbohydrates with molecular oxygen as benign oxidant has attracted considerable attention from the viewpoint of green sustainable chemistry.[1] This chemical process is mainly carried out over supported noble metal catalysts-for example, gold, palladium, rhodium, and ruthenium.[2] However, the high price, limited availability and potential toxity of these noble metals have spurred interest in catalysis with more earth-abundant and bio-relevant metals alternatives.[3] Iron is one of the ideal metal elements. It is the second most abundant metal in the earth crust and relatively non-toxic. In heterogeneous catalysis, iron oxides have important applications in ammonia synthesis, water gas shift and Fischer-Tropsch process.[4] Unfortunately, most of iron oxides catalysts work under drastic conditions (>300℃ and high pressure). Under comparably mild condition, they are catalytically inactive for the oxidation of alcohols using molecular oxygen as terminal oxidant.[5]

Downsizing the particles to nano- or subnanometre is a promising strategy to change the performance of catalysts.[6] In a preliminary work, we used a HNO_3-treated CMK-3 mesoporous carbon as supports to control the particle size of iron oxides, and firstly detected that supported ultrafine-iron-oxide (< 2 nm) displays a certain activity in selective oxidation of benzyl alcohol with air as oxygen source.[7] The intrinsic properties of carbon support seem to be important factors in the catalyst design. However, the concrete role of these factors, especially pore structure and surface properties, in the formation of catalytic active sites is still unclear. Moreover, carbon material is rather inert. Using post-modification method with oxidizing agents, the concentration of surface functional group is terribly low and the pore structure could also be damaged.[8, 9] These have become limitation of designing high-performing catalysts and identifying the underlying mechanism of supported ultrafine-iron-oxide catalysts.

Herein, we adopted a straightforward method for the fabrication of mesoporous carbon with abundant surface functional groups and tunable pore size. Using these carbons as supports, the activity of supported iron oxide catalysts was obviously enhanced. The catalysts can even work at as low as 40℃ and 1 atm air pressure, exhibiting an excellent capability to activate molecular oxygen. The relationship between nature of the carbon supports and the activity of resultant catalysts was investigated in detail. It clearly shows that the efficient carbon supports change not only the physical but also the chemical properties of iron oxide, and create new active sites for the catalytic process.

Results and discussion

Scheme 1 illustrates the preparation of mesoporous carbon (MC) and the supported ultrafine-iron-oxide catalysts (FeO_x/MC). MC was prepared using a modified hard-template

[a] Key Laboratory of Surface and Interface Chemistry of Jilin Province, College of Chemistry, Jilin University, Changchun, P. R. China
E-mail: lgang@jlu.edu.cn
[b] State Key Laboratory of Inorganic Synthesis and Preparative Chemistry, College of Chemistry, Jilin University, Changchun, P. R. China

† Electronic supplementary information (ESI) available: Experimental and characterization. See DOI: 10.1039/b000000x/

method involving carbonizing a kind of organic-inorganic composite containing citric acid, sugar, aluminum and phosphous ions, followed by removing in-situ formed aluminophosphate (AlPO) template[10] (see the Supporting Information for the detailed synthesis procedure). MC presents amorphous mesoporous character and relatively high surface area (Fig. 1A, Table S1). Three types of MC with the average pore size of 6.5, 3.8 and 2.9 nm could be obtained by tuning the ratio of citric acid to sugar in the organic-inorganic composite, which were denoted as MC-1, MC-2 and MC-3. Large amount of functional groups (including carboxylic, lactonic and phenolic groups) was detected on the surface of MC (total amount is about 3.0 mmolg^{-1}, Table S2), which is much higher than that of HNO_3-treated mesoporous carbon CMK-3 (H-CMK-3, 1.47 mmolg^{-1}), carbon nanotube (H-CNT, 0.20 mmolg^{-1}) and commercial active carbon (H-AC, 1.01 mmolg^{-1}). The in-situ formed AlPO contributes to the formation of large amount of surface functional groups. A suitable interaction present between carbon network and AlPO template, which is mainly originated from the coordination of citric acid with aluminium ions in the organic-inorganic complex.[10a] This interaction could restrain the complete pyrolysis of carbon precursors during carbonization, and this part of precursors was turned to surface functional groups after removing AlPO template.

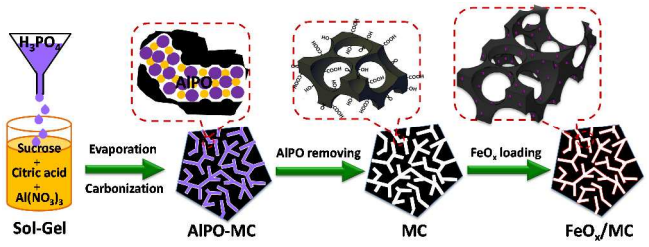

Scheme 1 Schematic illustration of the synthesis route used to prepare mesoporous carbon (MC) and supported iron oxide catalyst (FeO_x/MC).

MC was used as support to prepare supported iron oxides catalysts. Simple wet impregnation method was carried out using $Fe(NO_3)_3$•$9H_2O$ as iron precursor, and the loading amount of iron oxides was calculated with Fe_2O_3. The obtained solids were calcined at 673 K for 4 h in Ar flow, and the resultant material was denoted as x wt%FeO_x/MC. XRD patterns show that these samples exhibit two broad peaks assigned to diffractions from the (002), (100) graphite planes of MC support (Fig. S1). No crystalline phase related to iron oxide species could be observed, indicating that the particle size of iron oxides is very small. N_2 adsorption-desorption isotherms shows that all samples maintain the mesoporous structure of MC supports (Fig. 1B). The surface area and pore volume is a little lower than that of corresponding MC support (Table S1). It also suggests the high stability of the MC carbon supports.

All the prepared catalysts were tested in selective oxidation of benzyl alcohol with air as oxidant source (Table 1). It shows that neither bulk Fe_2O_3 nor MC supports obtained under the same preparation condition are active in this reaction (Table 1, entry 11 and 12). The catalysts prepared with HNO_3-treated commercial

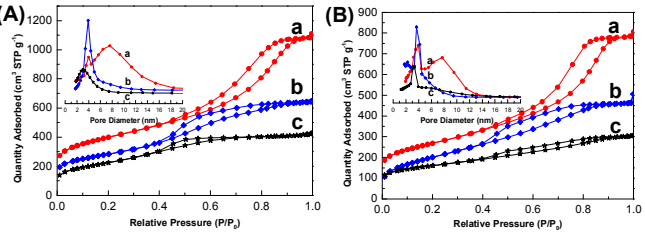

Fig. 1 N_2 adsorption-desorption isotherms of (A) MC supports: (a) MC-1, (b) MC-2, (c) MC-3 and (B) the supported iron oxide catalysts: (a) 5wt% FeO_x/MC-1, (b) 5wt% FeO_x/MC-2, (c) 5wt% FeO_x/MC-3. Inset shows the corresponding pore size distributions.

carbon as supports display relatively low activity. The conversions of benzyl alcohol on these catalysts are less than 60% after 8 h reaction (Table 1, entry 5-7). Under the same reaction condition, all 5wt%FeO_x/MC catalysts with different pore size exhibit a benzyl alcohol conversion of more than 92% (Table 1, entry 1-3). This result is much higher than that of the catalyst using HNO_3-treated CMK-3 as support (71.8 % conversion of benzyl alcohol, Table 1, entry 4). And the selectivity to benzaldehyde is nearly 100%. No other products such as benzoic acid and/or benzophenone were detected by GC-MS. TOF of 5wt%FeO_x/MC-1 is 6.10 h^{-1}, which is much higher than other carbon-supported metal oxide catalysts (Table S3). For ensuring the heterogeneous nature of the catalyst, a hot filtration test was performed (Fig. S3). After filtration, the sample originally containing FeO_x/MC showed no detectable subsequent conversion in the filtrate. Besides, the reusability of the FeO_x/MC was also tested. The catalyst can be used more than four cycles and the activity has no obviously decrease (Fig. S4). In a further study, we conducted the reaction at an even lower temperature (Table 1, entry 9-10). A 41.2% conversion was still achieved at reaction temperature of 40 ℃. To illustrate the general

Table 1 Catalytic activity of various catalysts for the air oxidation of benzyl alcohol.[a]

Entry	Catalyst	FeO_x [b]	Temp. [℃]	Conv. [%]	Select. [%]
1	FeO_x /MC-1	5 wt%	80	95.2	>99
2	FeO_x /MC-2	5 wt%	80	92.2	>99
3	FeO_x /MC-3	5 wt%	80	92.1	>99
4	FeO_x /H-CMK-3	5 wt%	80	71.8	>99
5	FeO_x /BP-2000	5 wt%	80	54.0	>99
6	FeO_x /H-AC	5 wt%	80	36.0	>99
7	FeO_x /H-CNT	5 wt%	80	5.9	>99
8	FeO_x /MC-1	0.25 wt%	80	32.8	>99
9	FeO_x /MC-1	5 wt%	60	69.1	>99
10	FeO_x /MC-1	5 wt%	40	41.2	>99
11	MC-1	—	80	14.9	>99
12	Fe_2O_3	—	80	0.9	>99

[a] Reaction conditions: benzyl alcohol (1 mmol), catalyst (0.3 g), solvent (toluene 10 mL), air 1 bar, reaction time 8 h. [b] The loading amount of FeO_x was calculated with Fe_2O_3.

applicability of FeO_x/MC, the catalyst was extended to air oxidation of as many as nine benzyl alcohol derivatives, and the results are presented in Table 2. 5wt%FeO_x/MC-1 also showed nice activity on the air oxidation of these benzyl alcohol derivatives, including *p*-nitro benzyl alcohol, *p*-chlorobenzyl alcohol, and 4-Hydroxy-3-methoxybenzyl alcohol.

Table 2 Catalytic oxidation of aromatic alcohols over 5wt% FeO_x/MC-1.[a]

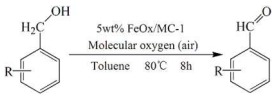

Entry	Substrate	Product	Yield [%]
1	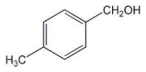	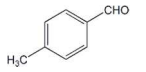	81%
2	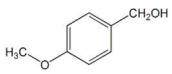	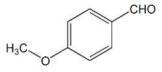	85%
3	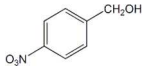	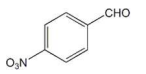	91%
4	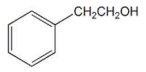	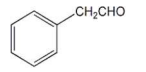	73%
5[b]	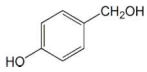	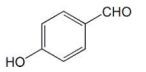	66%
6	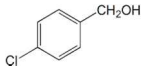	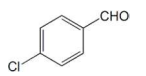	88%
7	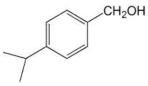	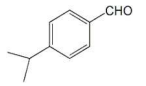	83%
8	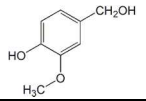	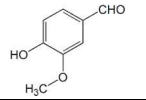	86%

[a] Reaction conditions: alcohols (1 mmol), catalyst (0.3 g), solvent (toluene 10 mL), 80 ℃, air 1 bar, reaction time 8 h. [b] Temperature 100 ℃.

TEM and HAADF-STEM images show a nearly homogeneous dispersion of iron oxide species, and no isolated particles present in the whole detected region of 5wt%FeO_x/MC-1 sample even under high resolution (Fig. 2a-2d). For making clear the composite unit of iron oxide species, a sample with 0.25wt% FeO_x loading amount was obtain by the same method. This sample is active in the title reaction (Table 1, entry 8). From the HAADF-STEM image, a few small iron oxide spots (about 2 nm) could be distinguished (Fig. 2f). While no isolated aggregated particles can be find in the corresponding HRTEM image. This result shows that iron oxide should present with much finer species, which is less than 2 nm.

From HRTEM images, it can be seen that FeO_x/MC catalysts possess disordered but uniform-size mesoporous structure (Fig. 2c). The pore size is about 5.0 nm, which is consistent with the result of N_2-adsorption. It should be an advantage for MC supports comparing with other carbon supports. These interconnected mesopores could facilitate the diffusion of reagent and product molecular.[11] As for the significant enhancement of catalytic performance, this might be a necessary but not a sufficient condition since the activity changes little with the pore size of MC supports increasing from 2.9 to 6.5 nm (Table 1, entry 1-3). The intrinsic properties of active sites and the formation mechanism should be focused to understand the high catalytic performance of FeO_x/MC. Temperature programmed reduction (TPR) in a H_2/Ar stream was carried out to detect the reducibility of the ultrafine-iron-oxide catalysts (Fig. S5). It shows that these iron oxide species are facilely reduced comparing with bulk and even nano-size iron oxides. This reflects that the iron oxides in the FeO_x/MC catalysts are facile changing the oxidation state, which should have direct correlation with their high catalytic performance.

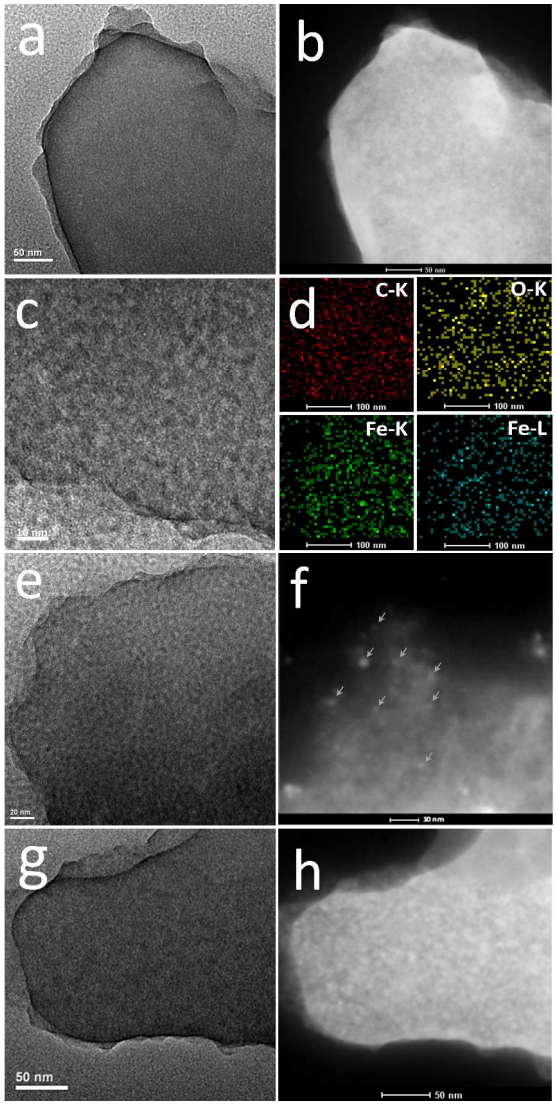

Fig. 2 HRTEM, HAADF-STEM and EDX mapping images of 5wt% FeO_x/MC-1 (a-d) and HRTEM and HAADF-STEM images of 0.25wt% FeO_x/MC-1 (e, f) and 5wt% FeO_x/ MC-R (g, h).

To understand the role of surface oxygen functional groups in constructing iron oxide active sites, three additional supports with different amount of surface oxygen functional groups were prepared

by treating MC-1 with following methods: alkali treated with 2 M NaOH aqueous solution (denoted as MC-Na); thermal treated in Ar at 800 ℃ for 6 h (denoted as MC-T); reduced in 5% H_2/Ar at 800 ℃ for 6 h (denoted as MC-R). DRIFT spectra show that the intensity of the bands centered at 1630 cm^{-1} (C=O stretch) and at 1350 cm^{-1} (C-O stretch)[12] decrease for the samples after treatment, especially for MC-T and MC-R (Fig. S6). It can qualitatively reflect the decrease of surface oxygen functional groups on these samples. The quantitative change was obtained by Boehm titration analysis. As shown in Fig. 3, the total amount of surface oxygen functional groups follows the trend MC-1 (3.23 mmol·g^{-1}) > MC-Na (1.52 mmol·g^{-1}) > MC-T (1.28 mmol·g^{-1}) > MC-R (0.78 mmol·g^{-1}). The amount of carboxylic and lactonic groups decreases significantly after these treatments.

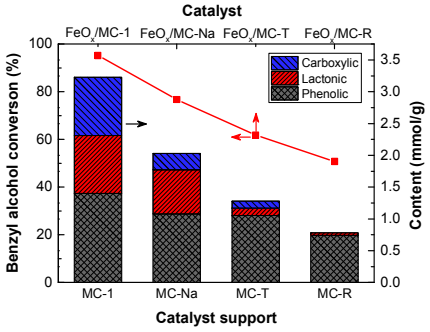

Fig. 3 Relationship between the amount of surface functional groups (phenolic, carboxylic and lactonic) on the carbon supports and the catalytic performance of the resultant catalysts. Reaction conditions: benzyl alcohol (1 mmol), catalyst (0.3 g), solvent (toluene 10 mL), air 1 bar, reaction time 8h.

All these samples were used as supports for preparing iron oxide catalysts (5 wt% loading amount), and the resultant catalysts were denoted as FeO_x/MC-Na, FeO_x/MC-T and FeO_x/MC-R, respectively. XRD patterns and Raman spectra show that all these samples have similar amorphous structure to FeO_x/MC-1 (Fig. S7). The BET surface area and porous properties of them is slightly different comparing with FeO_x/MC-1 (Table S4). The reactivity trend in this system follows FeO_x/MC-1 > FeO_x/MC-Na > FeO_x/MC-T > FeO_x/MC-R (Fig. 3). This result shows that the reactivity of final catalysts appear to be more in line with the amount of the oxygen functional groups on the surface of carbon support.

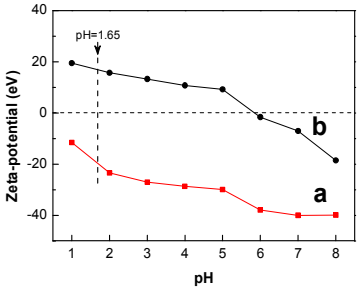

Fig. 4 Zeta-potentials of (a) MC-1 and (b) MC-R. The pH value is the preparation condition of iron nitrate impregnation.

As for FeO_x/MC-R, although no obvious particles were found in the HRTEM image, some aggregation should occur in this sample due to a few relatively bright spots can observed in its STEM image (Fig. 2g and 2h). Combined with the surface property of MC-R, it can further confirm the contribution of surface oxygen functional groups to the dispersion of iron oxides. Zeta-potential measurement was carried out to detect the surface charge properties of representative carbon supports. It shows that the oxygen functional groups render the MC-1 support surface negatively charged over a wide range of pH condition (Fig. 4a). The pH value of iron nitrate impregnation maintained at about 1.65 in our case. Under such preparation condition, an electrostatic force presents between the positively charged Fe^{3+} ions and negative carbon surface. The surface oxygen functional groups should serve as strongly active sites for anchoring Fe^{3+} ions, resulting in high dispersion of ultrafine iron oxide particles on MC-1 surface.

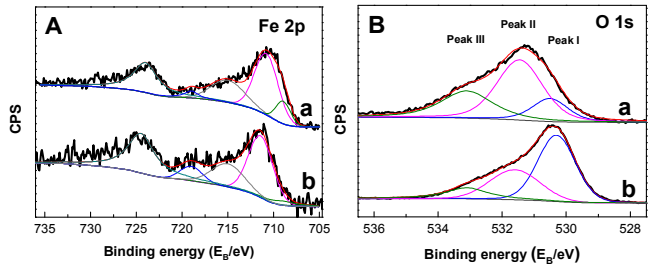

Fig. 5 Normalized Fe 2p (A) and O 1s (B) XPS spectra of (a) 5wt%FeO_x/MC-1 and (b) 5wt%FeO_x/ MC-R.

The chemical states of Fe and O on the surface of FeO_x/MC-1 and FeO_x/MC-R were determined by X-ray photon spectroscopy (XPS, Fig. 5). As shown in Fig. 5A, Fe (2p) core level is split into $Fe2p_{1/2}$ and $Fe2p_{3/2}$ due to spin orbit coupling. The main photoemission lines in the Fe 2p spectrum recorded from FeO_x/MC-1 appear at lower binding energy than those of the spectrum of FeO_x/MC-R, indicating the average Fe oxidation state in FeO_x/MC-1 is lower than that of Fe in FeO_x/MC-R. The spectra of $Fe2p_{3/2}$ can be fitted to two spin-doublets assignable to Fe^{3+} (centered at 711 eV) and Fe^{2+} (centered at 708.9 eV).[13] The amount of Fe^{2+} in FeO_x/MC-1 is obviously larger than that in FeO_x/MC-R. As for O1s spectra, an increase in the binding energy was found in FeO_x/MC-1 comparing with that of FeO_x/MC-R, indicating the presence of relatively strong interaction between iron oxide and MC-1 support. The O1s spectra can be deconvoluted into three peaks (Fig. 5B). Peak I at 530.3 eV attributed to the contribution of anionic oxygen in iron oxides.[14] Peak III at 533 eV can be attributed to the oxygen functional groups remained on the surface of catalysts.[15] Peak II at about 531.5 eV attributed to the interface oxygen origin from carboxylate O coordinated with Fe.[16] The relative amount of these oxygen species is obviously larger in FeO_x/MC-1 than that in FeO_x/MC-R. This binding energy is quite similar to the ligands surround central metals in homogeneous catalysis.[17] The abundant oxygen functional groups on the surface of MC-1 supports should provide a coordinate environment for ultrafine-iron-oxide species. The oxygen groups increase the electron density of iron centres, which promotes the formation of active sites for the oxidation of benzyl alcohol with molecular oxygen.

Conclusions

In summary, mesoporous carbons with abundant surface functional groups and tunable pore size have been obtained with a modified hard-template route. Using these carbons as supports, the resultant supported iron-oxide catalysts exhibit an enhanced activity in air oxidation of various benzyl alcohols. The amount of surface oxygen functional groups of carbon supports is the crucial factor for the dispersion of iron oxide species and the high activity of resultant catalyst. The negatively charged oxygen functional groups serve as strongly active sites for anchoring positively charged Fe^{3+} ions and result in high dispersion of ultrafine-iron-oxide particles. These functional groups also provide a suitable coordinate environment for ultrafine-iron-oxide, increasing the electron density of iron centres and forming of active sites for the oxidation of benzyl alcohol with molecular oxygen. This work shows that high performance iron oxide catalysts can be obtained by rational design of carbon support. This general strategy can also be extended to prepare other supported transition-metal-oxide catalysts with ultrafine particle size and high catalytic performance.

Acknowledgements

This work was financially supported by the National Natural Science Foundation of China (21473073, 21473074), the Development Project of Science and Technology of Jilin Province (20130101014JC), the Fundamental Research Funds for the Central Universities and the Open Project of State Key Laboratory of Inorganic Synthesis and Preparative Chemistry.

Notes and references

1 a) T. Punniyamurthy, S. Velusamy and J. Iqbal. *Chem. Rev*., 2005,**105**, 2329; b) A. N. Campbell and S. S. Stahl. *Acc. Chem. Res.,* 2012, **45**, 851; c) C. Parmeggiani and F. Cardona. *Green. Chem*., 2012, **14**, 547; d) K. Schröder, B. Join, A. J. Amali, K. Junge, X. Ribas, M. Costas and M. Beller. *Angew. Chem. Int. Ed*., 2011, **50**, 1425; e) Z. Ye, L. Hu, J, Jiang, J. Tang, X. Cao and H. Gu. *Catal. Sci. Technol.*, 2012, **2**, 1146.

2 a) M. S. Sigman and D. R. Jensen. *Acc. Chem. Res*., 2006, **39**, 221; b) S. Vajda, M. J. Pellin, J. P. Greeley, C. L. Marshall, L. A. Curtiss, G. A. Ballentine and J. W. Elam. *Nat. Mater.,* 2009, **8**, 213; c) B. Karimi, D. Elhamifar, O. Yari, M. Khorasani, H. Vali, J. H. Clark and A. J. Hunt. *Chem. Europ. J*., 2012, **18**, 13520; d) H. N. Kagalwala, A. B. Maurer, I. N. Mills and S. Bernhard. *ChemCatChem*, 2014, **6**, 3018; e) A. Villa, G. M. Veith, D. Ferri, A. Weidenkaff, K. A. Perry, S. Campisi and L. Prati. *Catal. Sci. Technol.*, 2013, **3**, 394.

3 a) C. Zhang, P. Feng and N. Jiao. *J. Am. Chem. Soc*., 2013, **135**, 15257; b) D. Obermayer, A. M. Balu, A. A. Romero, W. Goessler, R. Luque and C. O. Kappe. *Green. Chem*., 2013, **15**, 1530; c) R. V. Jagadeesh, H. Junge, M-M. Pohl, J. Radnik, A. Brückner and M. Beller. *J. Am. Chem. Soc.,* 2013, **135**, 10776; d) S. Fleischer, S. Zhou, K. Junge and M. Beller. *Angew. Chem. Int. Ed.,* 2013, **52**, 5120; e) Y. Gao, D. Ma, G. Hu, P. Zhai, X. Bao, B. Zhu, B. Zhang and D. Su. *Angew. Chem. Int. Ed.,* 2011, **50**, 10236; f) A. Jha, D. Mhamane, A. Suryawanshi, S. M. Joshi, P. Shaikh, N. Biradar, S. Ogale and C. V. Rode. *Catal. Sci. Technol.*, 2014, **4**, 1771.

4 a) N. D. Spencer, R. C. Schoonmake and G. A. Somorjai. *Nature*, 1981, **294**, 643; b) C. Yang, H. Zhao, Y. Hou and D. Ma. *J. Am. Chem. Soc.,* 2012, **134**, 15814; c) K. M. Driller, H. Klein, R. Jackstell and M. Beller. *Angew. Chem. Int. Ed.,* 2009, **48**, 6041; d) A.-H. Lu, J.-J. Nitz, M. Comotti, C. Weidenthaler, K. Schlichte, C. W. Lehmann, O. Terasaki and F. Schüth. *J. Am. Chem. Soc.,* 2010, **132**, 14152.

5 a) H. J. Schulte, B. Graf, W. Xia and M. Muhler. *ChemCatChem,* 2012, **4**, 350; b) S. Guo, G. Zhang, Y. Guo and J. C. Yu. *Carbon,* 2013, **60**, 437; c) *C.* Pirola, C. L. Bianch, A. D. Michele, S. Vitali and V. Ragaini. *Catal. Commun.,* 2009, **10**, 823.

6 a) J. Lu, J. W. Elam, P. C. Stair and *Acc. Chem. Res.,* 2012, **46**, 1806; (b) M. M. Forde, L. Kesavan, M. I. Saiman, Q. He, N. Dimitratos, J. A. Lopez-Sanchez, R. L. Jenkins, S. H. Taylor, C. J. Kiely and G. J. Hutchings. *ACS Nano,* 2014, **8**, 957; c) G. Liu, X. Wang, X. Wang, H. Han and C. Li. *J. Catal.,* 2012, **29**3, 616; d) Y. Liu, C.-J. Jia, J. Yamasaki, O. Terasaki and F. Schüth. *Ange. Chem. Int. Ed.,* 2010, **49**, 5771.

7 L. Geng, X. Zhang, W. Zhang , M. Jia and G. Liu. *Chem. Commun.,* 2014, **5**0, 2965.

8 a) D. Su, *S.* Perathoner and G. Centi. *Chem. Rev.,* 2013**, 113**, 5782; (b) C. Galeano, J. C. Meier, V. Peinecke, H. Bongard, I. Katsounaros, A. A. Topalov, A. Lu, K. J. J. Mayrhofer and F. Schüth. *J. Am. Chem. Soc.,* 2012, **134**, 20457.

9 a) J. L. Figueiredo, M. F. R. Pereira, M. M. A. Freitas and J. J. M. Orfao. *Carbon,* 1999, **37**, 1379; b) J. Zhu, A. Holmen and D. Chen. *ChemCatChem,* 2013, **5**, 378.

10 a) G. Liu, Z. Wang, M. Jia, X. Zou, X. Zhu, W. Zhang and D. Jiang. *J. Phys. Chem. B,* 2006, **110**, 16953; b) G. Liu, Y. Liu, Z. Wang, X. Liao, S. Wu, W. Zhang and M. Jia. *Microp. Mesop. Mater.,* 2008, **116**, 439.

11 a) B. Fang, J. H. Kim, M-S. Kim and J-S. Yu. *Acc. Chem. Res.,* 2013, **46**, 1397; b) S. Shrestha, S. Asheghi, J. Timbro and W. E. Mustain. *Carbon*, 2013, **60**, 28; c) L. Zhang and X. W. (Divid) Lou. *Chem. Eur. J.,* 2014, **20**, 5219; d) Y. Deng, Y. Cai, Z. Sun, D. Gu, J. Wei, W. Li, X. Guo, J. Yang and D. Zhao. *Adv. Funct. Mater*., 2010, **20**, 3658; d) Y. Yang, X. Liu, J. Zhao, B. Shi, J. Liu and Q. Yang. *Angew. Chem. Int. Ed.,* 2012, **51**, 9164.

12 a) C. Gong, M. Acik, R. M. Abolfath, Y. Chabal and K. Cho. *J. Phys. Chem. C,* 2012, **116**, 9969; b) D. R. Dreyer, H. P Jia and C. W. Bielawski. *Angew Chem. Int. Ed.,* 2010, **49**, 6813; c) L. Geng, S. Wu, Y. Zou, M. Jia, W. Zhang, W. Yan and G. Liu. *J. Colloid.Interf. Sci.,* 2014, **421**, 71.

13 a) J. Yang, H. Zhang, M. Yu, I. Emmanuelawati, J. Zou, Z, Yuan and C. Yu. *Adv. Funct. Mater.,* 2014, **24**, 1354; b) M. Monti, B. Santos, A. Mascaraque, O. R. Fuente, M. A. Niño, T. O. Mentes, A. Locatelli, K. F. McCarty, J. F. Marco and J. Figuera. *J. Phys. Chem. C,* 2012, **116**, 11539; (c) J. Zhang, J.-O. Müller, W. Zheng, D. Wang, D. Su and R. Schlögl. *Nano Lett,* 2008, **8**, 2738.

14 a) E. Smit, M. M. Schooneveld, F. Cinquini, H. Bluhm, P. Sautet, F. M. F. Groot and B. M. Weckhuysen. *Angew. Chem. Int. Ed.,* 2011, **123**, 1622; b) M. D. Sanchez, P. Chen, T. Reinecke, M. Muhler and W. Xia. *ChemCatChem,* 2012, **4**, 1997.

15 a) Q. Zhuo, J. Gao, M. Peng, L. Bai, J. Deng, Y. Xia, Y. Ma, J. Zhong and X. Sun. *Carbon,* 2013, **52**, 559; b) I.-Y. Jeona, Y.-R. Shina, G.-J. Sohna, H.-J. Choi, S.-Y. Baea, J. Mahmooda, S.-M. Junga,J.-M. Seoa, M.-J. Kima, D. W. Chang, L. Dai and J.-B. Baeka. *PNAS,* 2012, **109**, 5588.

16 S. L. Tait, Y. Wang, G. Costantini, N. Lin, A. Baraldi, F. Esch, L. Petaccia, S. Lizzit and K. Kern. *J. Am. Chem. Soc.,* 2008, **130**, 2108.

17 a) H. Tsunoyama, N. Ichikuni, H. Sakurai and T. Tsukuda. *J. Am. Chem. Soc*., 2009, **131**, 7086; b) P. C. A. Bruijnincx, M. Lutz, A. L. Spek, W. R. Hagen, B. M. Weckhuysen, G. V. Koten and R. J. M. K. Gebbink. *J. Am. Chem. Soc.,* 2007, **129**, 2275.